



Fully automated AI-based splenic segmentation for predicting survival and estimating the risk of hepatic decompensation in TACE patients with HCC

Lukas Müller¹ · Roman Kloeckner¹ · Aline Mähringer-Kunz¹ · Fabian Stoehr¹ · Christoph Düber¹ · Gordon Arnhold¹ · Simon Johannes Gairing² · Friedrich Foerster² · Arndt Weinmann² · Peter Robert Galle² · Jens Mittler³ · Daniel Pinto dos Santos^{4,5} · Felix Hahn¹

Received: 19 January 2022 / Revised: 19 January 2022 / Accepted: 5 March 2022 / Published online: 8 April 2022
© The Author(s) 2022

Abstract

Objectives Splenic volume (SV) was proposed as a relevant prognostic factor for patients with hepatocellular carcinoma (HCC). We trained a deep-learning algorithm to fully automatically assess SV based on computed tomography (CT) scans. Then, we investigated SV as a prognostic factor for patients with HCC undergoing transarterial chemoembolization (TACE).

Methods This retrospective study included 327 treatment-naïve patients with HCC undergoing initial TACE at our tertiary care center between 2010 and 2020. A convolutional neural network was trained and validated on the first 100 consecutive cases for spleen segmentation. Then, we used the algorithm to evaluate SV in all 327 patients. Subsequently, we evaluated correlations between SV and survival as well as the risk of hepatic decompensation during TACE.

Results The algorithm showed Sørensen Dice Scores of 0.96 during both training and validation. In the remaining 227 patients assessed with the algorithm, spleen segmentation was visually approved in 223 patients (98.2%) and failed in four patients (1.8%), which required manual re-assessments. Mean SV was 551 ml. Survival was significantly lower in patients with high SV (10.9 months), compared to low SV (22.0 months, $p = 0.001$). In contrast, overall survival was not significantly predicted by axial and craniocaudal spleen diameter. Furthermore, patients with a hepatic decompensation after TACE had significantly higher SV ($p < 0.001$).

Conclusion Automated SV assessments showed superior survival predictions in patients with HCC undergoing TACE compared to two-dimensional spleen size estimates and identified patients at risk of hepatic decompensation. Thus, SV could serve as an automatically available, currently underappreciated imaging biomarker.

Key Points

- Splenic volume is a relevant prognostic factor for prediction of survival in patients with HCC undergoing TACE, and should be preferred over two-dimensional surrogates for splenic size.
- Besides overall survival, progression-free survival and hepatic decompensation were significantly associated with splenic volume, making splenic volume a currently underappreciated prognostic factor prior to TACE.
- Splenic volume can be fully automatically assessed using deep-learning methods; thus, it is a promising imaging biomarker easily integrable into daily radiological routine.

Keywords Hepatocellular carcinoma · Transarterial chemoembolization · Artificial intelligence · Splenic volume

✉ Felix Hahn
felix.hahn@unimedizin-mainz.de

¹ Department of Diagnostic and Interventional Radiology, University Medical Center of the Johannes Gutenberg University Mainz, Langenbeckst. 1, 55131 Mainz, Germany

² Department of Internal Medicine I, University Medical Center of the Johannes Gutenberg University Mainz, Mainz, Germany

³ Department of General, Visceral and Transplant Surgery, University Medical Center of the Johannes Gutenberg University Mainz, Mainz, Germany

⁴ Department of Radiology, University Hospital of Cologne, Cologne, Germany

⁵ Institute for Diagnostic and Interventional Radiology, Goethe-University Frankfurt am Main, Frankfurt, Germany

Abbreviations

AFP	Alpha fetoprotein
AST	Aspartate aminotransferase
BSA	Body surface area
CI	Confidence intervals
CT	Computed tomography
HBV	Hepatitis B virus
HCC	Hepatocellular carcinoma
HRs	Hazard ratios
OS	Overall survival
TACE	Transarterial chemoembolization

Introduction

Hepatocellular carcinoma (HCC) is the most common primary liver cancer worldwide, and it ranks second among diseases responsible for cancer-related deaths [1, 2]. More than 80% of HCCs develop as a consequence of liver cirrhosis [3]. Thus, most patients with HCC have two different diseases: HCC and liver cirrhosis. Hence, it is essential to assess both tumor burden and remnant liver function in making optimal treatment decisions [3, 4].

In addition to compromising liver protein synthesis, cirrhosis also leads to progressive changes in the splanchnic circulation [5]. During cirrhosis, continuous tissue re-organizations lead to an increase in portal pressure. Portal hypertension ultimately leads to the development of gastroesophageal varices, ascites, and splenic volume increases [6, 7]. Consequently, a high splenic volume is related to severe liver cirrhosis [8]. Accordingly, the splenic volume has been identified as a highly sensitive prognostic parameter for patients with HCC undergoing resection or tumor ablation [9–11]. In an initial study in patients with HCC that underwent transarterial chemoembolization (TACE), splenic volume was recently identified as a relevant prognostic factor [12]. Progression-free survival and hepatic decompensation were not investigated. Moreover, the sample size was small and spleen volume was assessed manually [12]. Manual splenic volume assessments on cross-sectional computed tomography (CT) images is a time-consuming task with a high risk of interrater variance [13]. Thus, it is not feasible in daily clinical routine.

Fortunately, recent developments in the field of artificial intelligence, particularly deep learning, have provided knowledge about automated organ segmentation and volume assessments. These automated algorithms can be readily integrated into clinical workflows in real time [14]. Hence, splenic volume might become an easily assessable and readily available prognostic factor for treatment planning and post-TACE follow-ups.

This study had two primary research goals: First, we aimed to build a deep-learning algorithm for fully automated splenic volume assessments based on CT images. Second, we aimed to validate the role of total splenic volume as a novel imaging

biomarker for survival prediction and to investigate its role as an indicator for hepatic decompensation in patients with HCC undergoing TACE.

Methods

The Ethics Committee of the Medical Association of Rhineland Palatinate, Mainz, Germany, approved this study (permit number 2021-15984). The requirement for informed consent was waived, due to the retrospective nature of the study. Patient records and information were anonymized prior to analysis. This report followed the guidelines for transparent reporting of a multivariable prediction model for individual prognosis or diagnosis (TRIPOD) and the guidelines for reporting observational studies (STROBE) (Supplementary Tables 1 and 2) [15, 16].

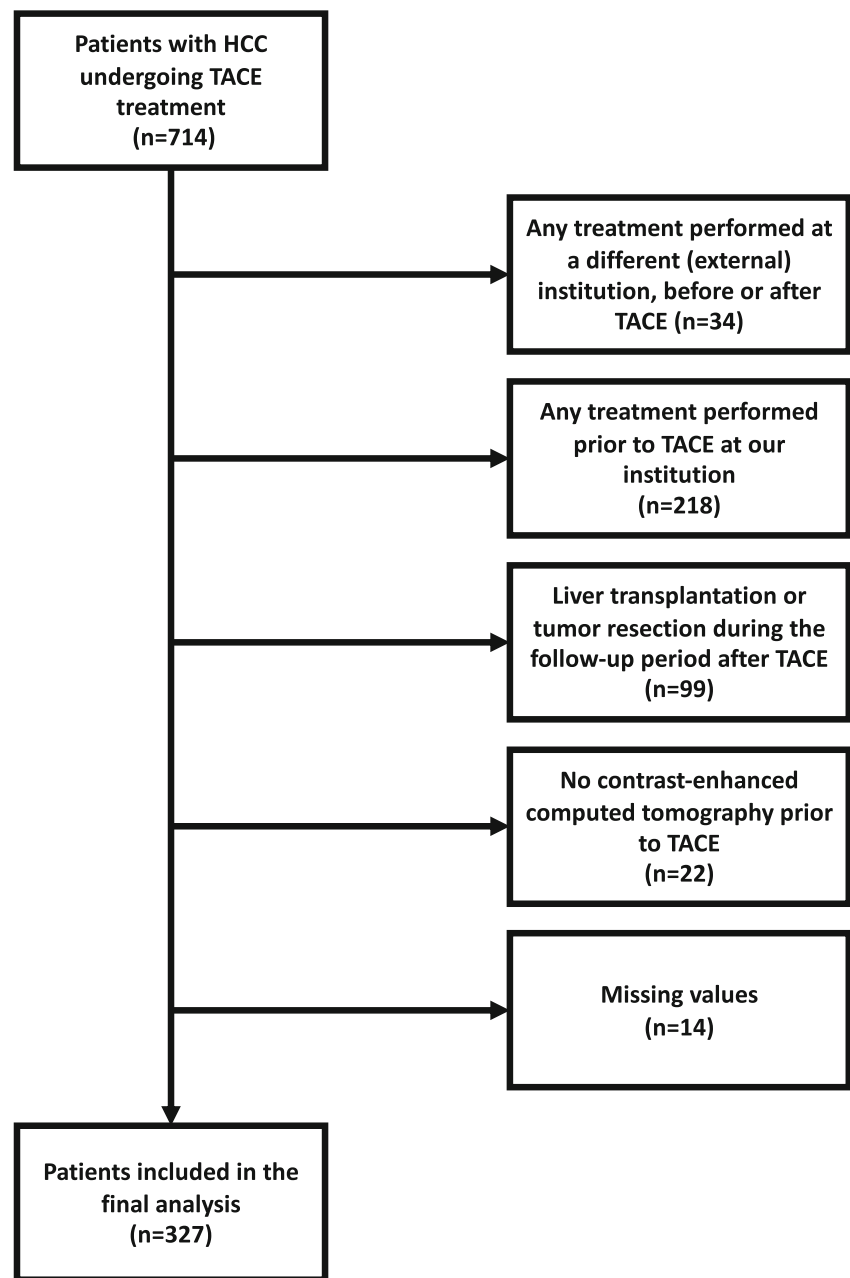
Patients

We identified 714 patients with confirmed HCC that received TACE treatment in our tertiary care center between January 2010 and November 2020. Of these, 327 patients fulfilled the following inclusion criteria: (1) age above 18 years; (2) histologically or image-derived HCC diagnosis based on the EASL criteria; (3) no treatment performed prior to TACE; (4) no liver transplantation or tumor resection during the follow-up period after TACE; (5) pre-interventional contrast-enhanced CT scan for splenic volume assessment; (6) full availability of clinical, laboratory, and imaging data. A total of 387 patients were excluded, due to reasons shown in Fig. 1.

Diagnosis, treatment, and follow-up

HCC was diagnosed, based on histological or image-derived criteria established by the European Association for the Study of the Liver, as previously described [3, 17]. All patients underwent contrast-enhanced CT for treatment planning. Indications for TACE were discussed in an interdisciplinary tumor board, which included hepatologists/oncologists, diagnostic and interventional radiologists, visceral surgeons, pathologists, and radiation therapists. TACE was performed in a standardized manner, as previously described [18, 19]. Follow-ups included cross-sectional imaging, a clinical examination, and blood sampling. Follow-ups were performed every 6 or 12 weeks, depending on the presence of viable tumor tissue [17]. Radiologic response was assessed using mRECIST criteria [3, 20]. The first primary endpoint was the median overall survival (OS), defined as the interval between the initial TACE session and the date of death or last follow-up. Moreover, we investigated hepatic decompensation after TACE, which was objectively defined as an increase of the ALBI grade 3 months after the initial TACE as

Fig. 1 Flowchart of the patient selection process for this study



previously proposed [21, 22]. Further endpoints were the time to progression (TTP) and the time to untreatable (unTACEable) progression (TTUP). UnTACEable progression is defined as a clinical status that prohibits further TACE [3]. This status is caused by non-response of target lesions after two or more TACE sessions, new extrahepatic tumor spread, or hepatic decompensation [23].

Data acquisition

The dataset was acquired from the clinical registry unit, as previously reported [17]. This dedicated, prospectively populated database contained data on all patients with primary liver

cancer [24]. Additional imaging and laboratory data were acquired from the radiology information system and the laboratory database. The final dataset included all available data on patient demographics, clinical assessments of the underlying liver disease and tumor, imaging, factors related to the TACE treatment, and laboratory parameters measured prior to the initial TACE treatment [17].

Splenic volume assessment: algorithm design, training, and validation

We used the open source Python library MIScnn (<https://github.com/frankkramer-lab/MIScnn>) to train an automated algorithm.

Table 1 Baseline patient characteristics

Variable	All patients (<i>n</i> = 327)
Median age, years (IQR)	69.1 (62.6–75.4)
Sex, <i>n</i> (%)	
Female	51 (15.6)
Male	276 (84.4)
Etiology, <i>n</i> (%) ^a	
Alcohol	156
Hepatitis C	55
Hepatitis B	28
NAFLD	26
Hemochromatosis	9
AIH/PBC/PSC	5
Unknown/other	27
Child-Pugh stage, <i>n</i> (%)	
A	120 (36.7)
B	133 (40.7)
C	30 (9.2)
No cirrhosis	44 (13.4)
BCLC stage, <i>n</i> (%)	
0	0
A	60 (18.3)
B	166 (50.8)
C	71 (21.7)
D	30 (9.2)
Median tumor size, mm (IQR)	42 (28–64)
Tumor number, <i>n</i> (%)	
Unifocal	74 (22.6)
Multifocal	221 (67.6)
Diffuse growth pattern	32 (9.8)
Median albumin level, g/l (IQR)	31 (27–35)
Median bilirubin level, mg/dl (IQR)	1.4 (0.8–2.2)
Median platelet count, per nl (IQR)	129 (87–192)
Median AST level, U/l (IQR)	64 (46–100)
Median ALT level, U/l (IQR)	41 (28–61)
Median INR (IQR)	1.2 (1.1–1.3)
Median AFP level, ng/ml (IQR)	30 (7–767)
Number of TACE sessions, <i>n</i> (%)	
Single	84 (25.7)
Multiple	243 (74.3)
Subsequent treatment	
Yes ^b	72 (22.0)
No	255 (78.0)

^a More than one etiology was possible for liver disease; thus, percentages were not calculated. Abbreviations: *NASH*, nonalcoholic steatohepatitis; *AIH*, autoimmune hepatitis; *PBC*, primary biliary cholangitis; *PSC*, primary sclerosing cholangitis; *BCLC*, Barcelona Clinic Liver Cancer; *AST*, aspartate aminotransferase; *ALT*, alanine aminotransferase; *AFP*, alpha fetoprotein. ^b Sorafenib (*n* = 33), lenvatinib (*n* = 13), selective internal radiation therapy (*n* = 12), atezolizumab in combination with bevacizumab (*n* = 6), pembrolizumab (*n* = 2), pembrolizumab in combination with regorafenib (*n* = 2), lenvatinib followed by sorafenib (*n* = 1), linifanib followed by sorafenib (*n* = 1), nivolumab (*n* = 1), ramucirumab (*n* = 1)

The library provides a convolutional neural network with a U-Net architecture, which allows the segmentation of 3D medical images [25]. Thus, we extracted the portal venous phase of the abdominal CT scans for all patients in our dataset. For the first 100 consecutive patients in the dataset, we manually segmented the spleen with the freely available LIFEx software (www.lifexsoft.org) [26]. However, as MIScn reads NIfTI image segmentation

files (<https://nifti.nimh.nih.gov/>), any segmentation software which is able to save in this format could have been used.

Next, we used the first 70 manually segmented spleens for training a spleen segmentation algorithm, and the remaining 30 manually segmented spleens to validate the neural network. Preprocessing of the images (resampling to $2 \times 2 \times 3$ mm, clipping from -50 to 350 to Hounsfield units, and Z-score normalization) and six cycles of data augmentation in the training set were performed as provided by the library. During training, the Tversky loss was calculated and we implemented Keras callback functions to facilitate early stopping and to reduce the learning rate on plateaus [27, 28]. Training was performed for 300 epochs. For postprocessing, we selected the largest connected region in the left half of the abdomen to avoid rare cases of erroneous partial liver segmentation.

After training, the portal venous phase CT scans of the remaining 227 patients were automatically processed by the algorithm without the need of further human preprocessing. We evaluated the results with graphic overlays of the predicted segmentation for these remaining 227 patients, and splenic volume was automatically calculated. The graphic overlays were used by two independent readers to rate the performance of the algorithm (i.e., perfect, acceptable, or poor). In cases of discrepancy, a consensus reading was performed. Patients with perfect or acceptable computed splenic segmentations were included in the statistical analyses; patients with a poor grade were assigned to manual segmentation for further analysis. Additionally, spleen volume in relation to the body surface area (BSA) was calculated, which was assessed using the patient's height and weight.

Axial and craniocaudal spleen sizes were manually assessed in a standardized manner, as previously described [13].

Statistical analysis

All statistical analyses and graphics were performed in R studio (RStudio Team [2020]. RStudio: Integrated Development for R. RStudio, PBC, <http://www.rstudio.com>, last accessed 30 Sept 2021) with R 4.0.3 (A Language and Environment for Statistical Computing, R Foundation for Statistical Computing, <http://www.R-project.org>; last accessed 10 Jan 2022). Binary and categorical baseline parameters are expressed as absolute numbers and percentages. Continuous data are expressed as the median and range. Subgroups were compared with the chi-square test and Mann-Whitney *U*-test. The Sørensen Dice Score was calculated to assess algorithm performance. Furthermore, manual and automated splenic volume assessments were compared with a Bland-Altman plot. Survival analyses were performed with the packages “survminer” and

“survival” (<https://cran.r-project.org/package=survminer>, <https://CRAN.R-project.org/package=survival>, last accessed 10 Jan 2022). Survival was evaluated with Kaplan–Meier curves, and strata were compared with log-rank testing. We used the same packages to determine cut-off values for splenic volumes, based on optimal stratification. We built univariate and multivariate Cox proportional hazards regression models and assessed hazard ratios (HRs) and the corresponding 95% confidence intervals (CIs). Sensitivity, specificity, and area under the curve (AUC) were calculated using the package “pROC” (<https://cran.r-project.org/web/packages/pROC/index.html>, last accessed 10 Jan 2022). The optimal cutoff for maximized sensitivity and specificity was determined using the Youden Index. p -values < 0.05 were considered statistically significant.

Results

Baseline

The baseline characteristics of patients with HCC at the initial TACE treatment are shown in Table 1.

Algorithm performance

The manual assessments yielded a mean splenic volume of 549.7 ml for the training dataset and 524.3 ml for the validation dataset. The algorithm assessments yielded a mean splenic volume of 550.8 ml for the training set and 512.6 ml for the validation set. The mean difference between the manual and algorithm volume assessments was 0.1%, with a standard deviation

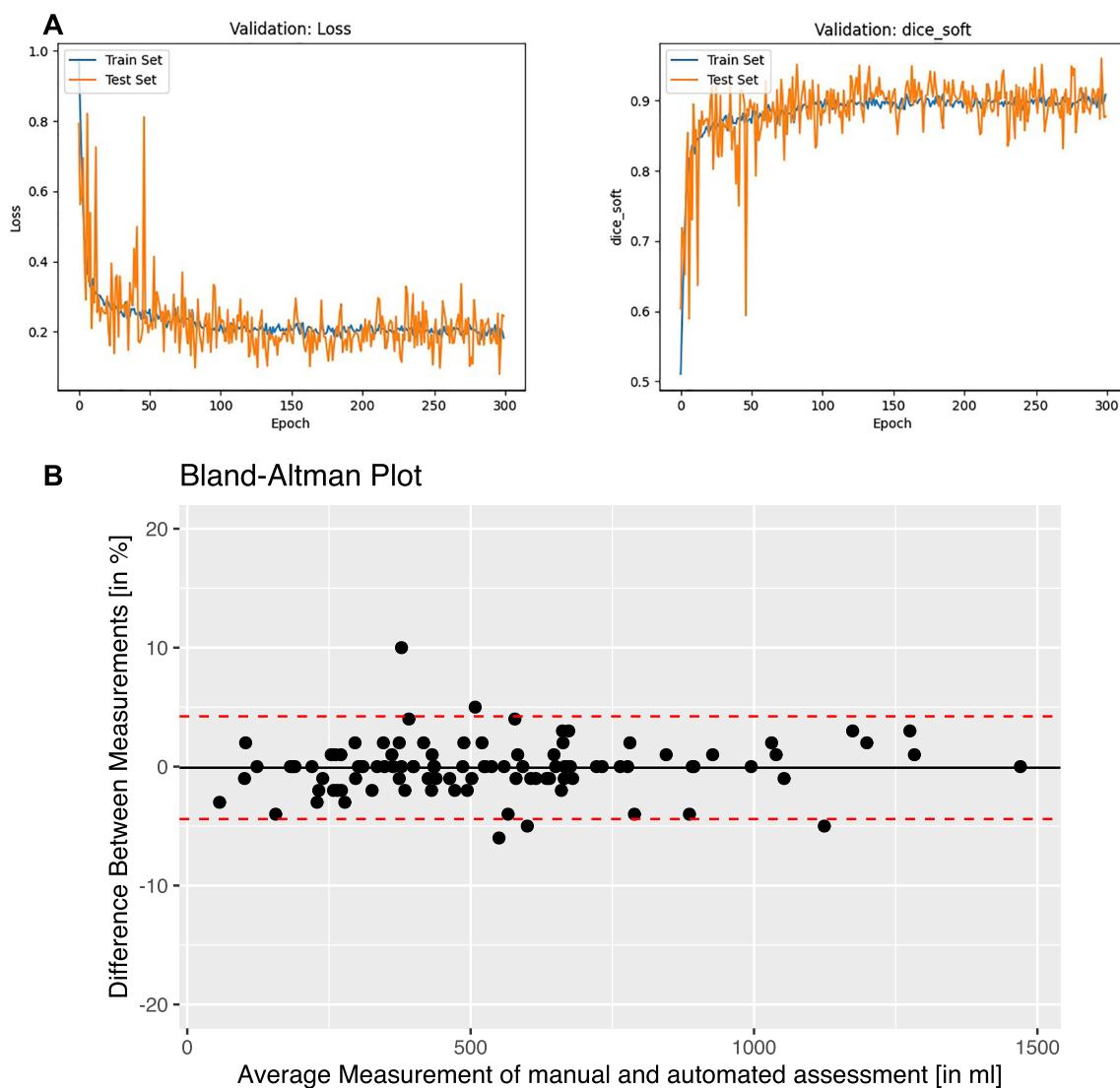


Fig. 2 The course of training of the convolutional neural network (**A**) ((left) Tversky loss values over the number of epochs; (right) Sørensen Dice Scores over the number of epochs; train set: 70 sets of manually

segmented spleen data; test set: 30 different sets of manually segmented spleen data); Bland-Altman Plot shows the distribution of manually and automatically assessed splenic volumes (**B**)

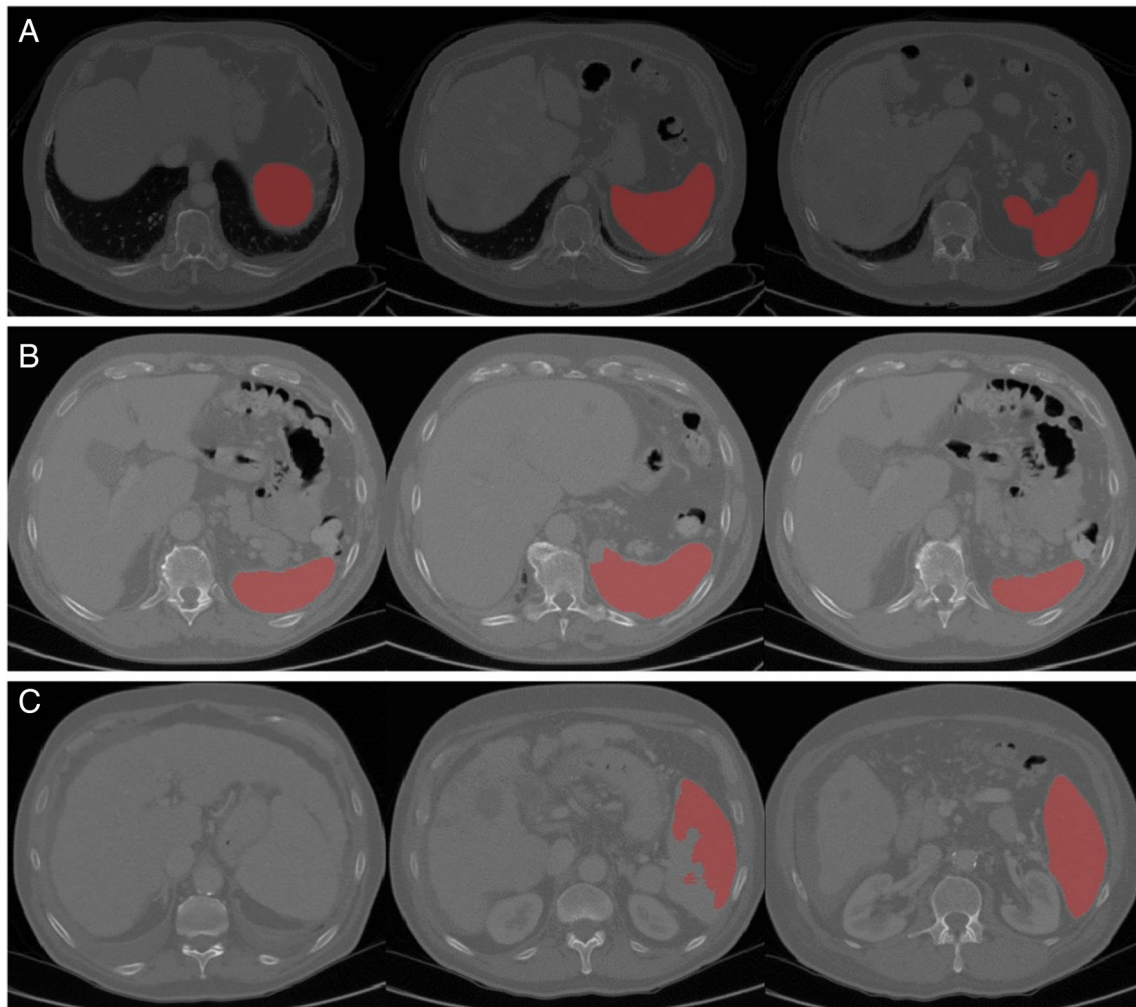


Fig. 3 Representative images of the algorithm's performance (from left to right images at upper, middle, and lower part of the spleen): **A** perfect segmentation, **B** acceptable segmentation (minor segmentation error

medially), **C** poor segmentation (major segmentation error in the upper part with kissing liver and spleen phenomenon)

of 2.2%. The training progress of the convolutional neural network is depicted in Fig. 2a; the distribution of volumes is shown in a Bland-Altman Plot in Fig. 2b. The Sørensen Dice coefficients were 0.96 for both the training and validation sets.

Next, we assessed the automated segmentation for the remaining patient cohort ($n = 227$). We found that 206 (90.7%) measurements were rated perfect, 17 (7.5%) were rated acceptable, and four (1.8%) were rated poor, after consensus reading. Representative images of each grade are shown in Fig. 3; the complete animation of each example is provided in the supplement (Supplementary Figs. S1a-S1c). For the four cases with poor ratings, we performed additional manual segmentations to obtain the proper splenic volume.

Splenic volume

The mean splenic volume for the whole patient cohort was 551.2 ml. In addition, the mean axial diameter was 132.3 mm

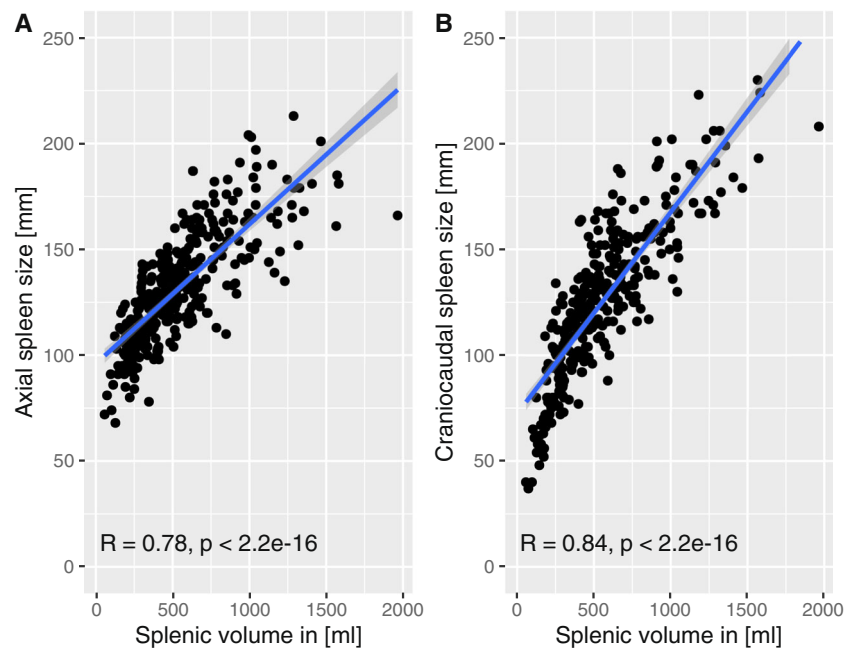
and the mean craniocaudal diameter 125.0 mm. Both the axial and craniocaudal diameters were significantly correlated with the splenic volume ($p < 0.001$, Fig. 4), with high Pearson coefficient values (0.78 and 0.84, respectively).

Survival analysis

Based on an optimal stratification of the median OS, we found that the best cut-off value for predicting mortality risk was a splenic volume of 382.6 ml. With this cut-off value, 219 (67.0%) patients had high splenic volumes and 108 (33.0%) had low splenic volumes. The median OS of patients with high and low splenic volumes were 10.6 and 18.8 months, respectively ($p = 0.014$, Fig. 5a).

The optimal stratifications of axial and craniocaudal spleen sizes yielded cut-off values of 163 and 115 mm, respectively. Neither index showed a significant association with OS in univariate analyses. The median OS

Fig. 4 Correlation between two-dimensional splenic measurements and splenic volume. **A** Axial spleen size; **B** craniocaudal spleen size



times were 9.9 and 13.1 months ($p = 0.220$) for high and low axial spleen diameters, respectively (Supplementary Fig. S2A), and 11.9 and 16.1 months ($p = 0.063$), for high and low craniocaudal spleen diameters, respectively (Supplementary Fig. S2B).

A univariate Cox hazard regression analyses identified a high splenic volume, low albumin, high bilirubin, high AST, and a large tumor size as significant prognostic factors (Table 2). None of the other included risk factors showed a significant association with OS. In the subsequent multivariate analysis, which included all the significant abovementioned factors, splenic volume did not reach significance.

Subsequently, we analyzed the role of the splenic volume normalized to BSA for all patients with available information on body weight and height ($n = 289$). Based on an optimal stratification of the median OS, we found that the best cut-off value for predicting mortality risk was a splenic volume-to-BSA ratio of 192.7 ml/m². With this cut-off value, 200 (69.2%) patients had high splenic volume-to-BSA ratio, and 89 (30.8%) had low ratio. The median OS of patients with high and low splenic volume-to-BSA ratio were 10.9 and 22.0 months, respectively ($p = 0.001$, Fig. 5b).

A univariate Cox hazard regression analyses identified a high splenic volume-to-BSA ratio, low albumin, high bilirubin, and a large tumor size as significant prognostic factor (Table 3). None of the other included risk factors showed a significant association with OS. In multivariate analysis, splenic volume-to-BSA ratio remained an independent prognostic predictor, as did the other abovementioned significant factors.

Furthermore, we analyzed TTP and TTUP of these patients with regard to the normalized splenic volume using the same cut-off value. The median TTP of patients with high and low splenic volume-to-BSA ratio were 6.7 and 11.1 months, respectively ($p = 0.10$, Supplementary Fig. S3A). The median TTUP of patients with high and low splenic volume-to-BSA ratio were 9.9 and 27.8 months, respectively ($p < 0.001$, Supplementary Fig. S3A).

Influence on subsequent treatment

The median splenic volume of patients who were able to receive multiple TACE sessions was significantly lower (458 ml vs 582 ml, $p < 0.001$). Furthermore, the median splenic volume of patients who received subsequent treatment was also significantly lower (399 ml vs 520 ml, $p < 0.001$).

Risk of hepatic decompensation

We further assessed the risk of an increase in the ALBI grade for patients who had an initial grade of 1 or 2 and an available follow-up ALBI value 3 months after TACE ($n = 197$, 60.2%). Of these patients, a total of 61 (31.0%) patients had an ALBI grade increase 3 months after TACE. The median splenic volume of these patients was significantly higher (632 ml, IQR 514–868 ml) in comparison to patients without an increase (363 ml, IQR 261–477 ml) ($p < 0.001$, Fig. 6). Receiver operating characteristic analysis revealed an AUC of 0.83 with a sensitivity of 91.2% and a specificity of 72.1% at the cut-off of 455.3 ml for predicting an ALBI increase.

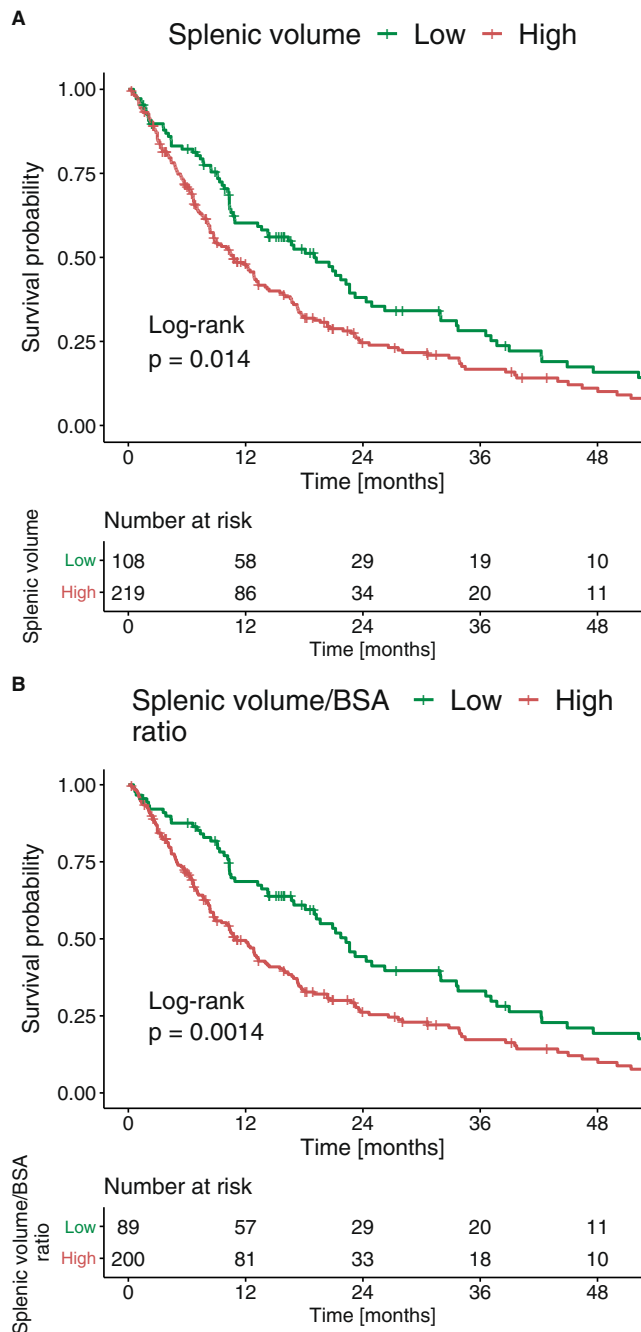


Fig. 5 **A** Kaplan–Meier survival curves show survival of patients with low (green) and high (red) splenic volumes ($n = 327$); **B** Kaplan–Meier survival curves show survival of patients with low (green) and high (red) splenic volume-to-BSA ratio ($n = 289$)

Discussion

This study was the first to assess the prognostic role of splenic volume for patients with HCC undergoing TACE in a Western patient cohort. Here, we developed a fully automated approach, based on deep-learning methods, for assessing splenic volume.

Manual assessments of splenic volume are time-consuming, and they run a high risk of interrater variance [13]. Thus, we built a deep learning–based tool to assess splenic volume automatically, based on CT images. The U-Net architecture used for segmentation yielded a Sørensen Dice coefficient of 0.96 for training and 0.96 for validation. These coefficients indicated excellent algorithm performance. Additionally, the manual and automatic splenic volume assessments only differed by 0.1%.

The time consumption and technical challenges of manual splenic volume assessments [13] have hindered their integration into clinical workflows, despite reports that splenic volume was a highly predictive factor for several cancer entities, including HCC [9–11]. Historically, several surrogates have been proposed for rapid estimations of splenic volume. For patients with liver cirrhosis, the axial and craniocaudal diameters of the spleen have been identified as precise surrogates of splenic volume [13]. Our results also indicated that these diameters were moderately to highly correlated with splenic volume. However, neither the craniocaudal nor the axial diameter was a relevant prognostic factor, because neither reached significance, even with optimal stratification, in our cohort. Thus, when deciding whether to use estimates for spleen size or true splenic volume for assessing risk in patients with HCC undergoing TACE, true splenic volume should be favored.

AI-based algorithms can potentially simplify the radiologist’s work in daily clinical routines [14]. Tasks that can be readily simplified and automatized include organ segmentation, volume assessments, and body composition assessments [29–31]. Recently, deep learning algorithms have also been used for the assessment of splenic volume in the context of variceal detection [32]. AI-based algorithms have the advantage of being easy to integrate into clinical workflows and automated quantitative reports can be automatically sent to the local image archiving and communication system. However, currently, those new technologies require evaluation in the context of clinical applications. Accordingly, specific use cases are mandatory.

While there is an initial threshold to install and train a segmentation tool, which includes a manual one-time labeling of a training dataset, this effort is reduced thanks to publicly available software programs and libraries. Using other software for segmentation and U-Nets than the ones used in this study would have likely produced similar effective results, and once trained, no further user segmentation is needed to get an accurate splenic volume.

The literature is scarce regarding the prognostic role of splenic volume for patients with HCC undergoing TACE. To date, only one recent study by Dai et al showed that splenic volume was correlated to the Child-Pugh classification and OS [12]. The mean splenic volume of the 67 patients in that

Table 2 Univariate and multivariate Cox regression results of factors related to survival for all patients ($n = 327$)

Covariate	Category	Univariate			Multivariate		
		HR	95% CI	<i>p</i> -value	HR	95% CI	<i>p</i> -value
Age	≥ 70 years	1.0	0.8–1.3	0.920			
AFP	> 400 ng/ml	1.0	0.7–1.2	0.770			
Albumin level	≥ 35 g/l	2.2	1.7–2.9	< 0.001	1.7	1.3–2.4	< 0.001
Bilirubin level	≥ 1.2 mg/dl	2.1	1.7–2.8	< 0.001	2.0	1.5–2.6	< 0.001
AST level	> 31 U/l	1.8	1.1–3.1	0.033	1.8	1.0–3.2	0.047
ALT level	≥ 35 U/l	1.2	0.9–1.6	0.190			
INR level	> 1.2	1.1	0.8–1.4	0.550			
Platelet count	> 100 /ml	1.0	0.8–1.3	0.850			
Tumor number	≥ 2	1.3	0.9–1.7	0.150			
Max. lesion size	> 5.0 cm	1.3	1.0–1.8	0.037	1.4	1.0–3.2	0.028
Splenic volume	High	1.4	1.1–1.8	0.014	1.1	0.9–1.5	0.354
Axial spleen size	High	1.2	0.9–1.8	0.220			
Cranio-caudal spleen size	High	1.3	1.0–1.7	0.064			

Significant *p* values are marked in bold

HR hazard ratio, CI confidence interval, AFP alpha fetoprotein, AST aspartate aminotransferase, ALT alanine aminotransferase

study was 300 ml, prior to TACE. That value was considerably lower than the mean volume of 551 ml in our patient cohort. In contrast to our study, the underlying etiology in all their patients was hepatitis B virus (HBV) infection. Unfortunately, they did not provide the number of patients with underlying cirrhosis. In general, most patients with chronic HBV infections and HCC do not have underlying cirrhosis. Thus, those patients are at lower risk of developing signs of portal hypertension, like an increased splenic volume. Accordingly, in that study, a smaller proportion of patients were in the high Child-Pugh class, compared to our cohort.

Thus, those patients had better average liver function than the patients included in our study. All these factors might have explained the higher splenic volume in our patient cohort. Nevertheless, the two studies reported similar optimal cut-off values (373 ml vs 383 ml in our study) for high and low splenic volume.

Splenic volume was also significantly associated with both progression-free survival as well as hepatic decompensation and the likeliness to receive subsequent systemic treatment after TACE failure in our cohort. This is in line with prior findings that progression-free survival in TACE patients is

Table 3 Univariate and multivariate Cox regression results of factors related to survival for patients with available body surface area ($n = 289$)

Covariate	Category	Univariate			Multivariate		
		HR	95% CI	<i>p</i> -value	HR	95% CI	<i>p</i> -value
Age	≥ 70 years	1.0	0.8–1.3	0.950			
AFP	> 400 ng/ml	1.0	0.7–1.2	0.700			
Albumin level	≥ 35 g/l	2.2	1.6–3.0	< 0.001	1.8	1.3–2.5	< 0.001
Bilirubin level	≥ 1.2 mg/dl	2.1	1.6–2.8	< 0.001	1.9	1.4–2.5	< 0.001
AST level	> 31 U/l	1.7	1.0–2.9	0.064			
ALT level	≥ 35 U/l	1.2	0.9–1.6	0.220			
INR level	> 1.2	1.1	0.8–1.5	0.650			
Platelet count	> 100	1.0	0.8–1.3	0.910			
Tumor number	≥ 2	1.2	0.9–1.7	0.190			
Max. lesion size	> 5.0 cm	1.3	1.0–1.8	0.045	1.4	1.1–1.9	0.017
Splenic volume/BSA ratio	High	1.6	1.2–2.2	0.002	1.4	1.0–1.9	0.046

HR hazard ratio, CI confidence interval, AFP alpha fetoprotein, AST aspartate aminotransferase, ALT alanine aminotransferase, BSA body surface area

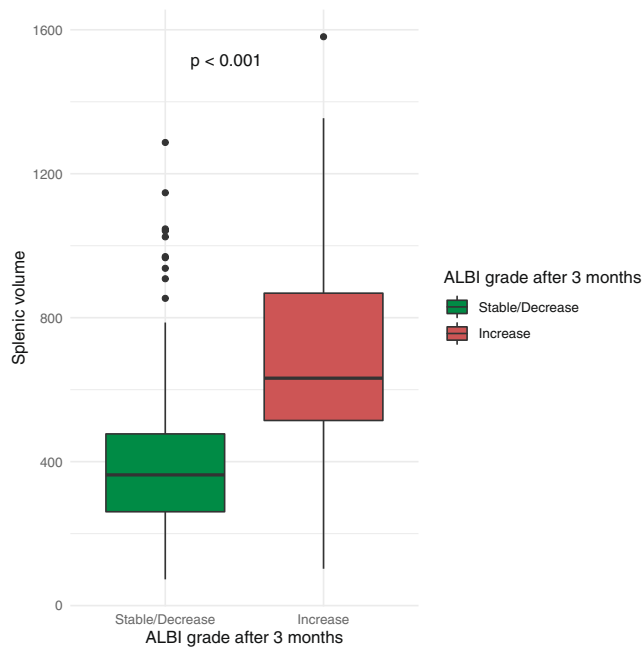


Fig. 6 Boxplot showing the distribution of the splenic volume among patients with a stable/decrease ALBI grade (green) and patients with an increased ALBI grade (red) 3 months after TACE

linked to portal hypertension [33]. Moreover, prior studies have linked repeated TACE to an increase in portal hypertension [34] and have described the ALBI score as a predictor for failure of sorafenib treatment [35, 36].

In our study, we found that splenic volume prior to TACE has a high sensitivity of identifying patients with a post-treatment ALBI increase. Therefore, our study is the first identifying splenic volume as relevant prognostic imaging marker for hepatic decompensation in patients with unresectable HCC. In the context of emerging novel treatment options for patients with unresectable HCC, the optimal time-point for a treatment switch in the concept of stage migration is hard to identify [37]. However, a treatment switch is of utmost importance for the outcome of the patients as “an inappropriately high number of TACE sessions delays the switch to systemic therapy and may, in some cases, completely hinder the treatment switch due to the deterioration of liver function” [38]. Thus, splenic volume might function as an additional, currently underused parameter to identify patients at high risk for hepatic decompensation and therefore might lead to a tighter follow-up scheme and more frequent interdisciplinary discussion of these patients. However, no standard reference values neither for impaired survival nor increased risk of hepatic decompensation are currently available. Thus, future large-scale multicentric evaluation studies are needed to determine a generalizable cut-off value.

The present study had several limitations. First, it was a single-center, retrospective study. However, the sample size was distinctly larger than that included in the previous study

on this topic [12]. Additionally, our dataset was well investigated and we only included patients with complete clinical, laboratory, and imaging data. Furthermore, missing values were not imputed. To avoid a time bias, we actively decided to include only patients from 2010 and later. These criteria minimized differences in the diagnosis and treatment decisions, which provided a more homogeneous study cohort. Furthermore, we excluded patients that underwent previous treatments to avoid other biases. Second, we included patients that underwent either conventional or drug-eluting bead-delivered TACE. However, several previous studies have shown that the TACE delivery technique did not influence the OS [39–41]. Third, we only used an internal validation set to assess algorithm performance. In the final prediction for the whole dataset, the neural network failed to provide an accurate prediction of splenic volume in four patients (1.8%). We restricted the training and validation cohort to 100 patients, determined a priori, to limit the burden of manual segmentation. Nevertheless, the neural network facilitated correct splenic volume calculations in 98.2% of non-segmented spleens. Therefore, the evaluation of this use case was not substantially hindered by the need to perform additional manual segmentations of those four spleens with grotesque anatomies. Consequently, we encourage future studies to employ neural networks for segmentation in validating the prognostic role of splenic volume for patients with HCC undergoing TACE.

In summary, we showed that training a deep learning algorithm was feasible for allowing fully automated splenic volume assessments for patients with HCC undergoing TACE. Compared to established two-dimensional estimates of splenic volume, our algorithm provided precise splenic volume assessments, which showed superiority in predicting survival and high sensitivity in identifying patients with a risk of hepatic decompensation. Thus, true splenic volume could serve as an additional imaging biomarker, available fully automatically without additional effort for every CT study.

Supplementary Information The online version contains supplementary material available at <https://doi.org/10.1007/s00330-022-08737-z>.

Acknowledgements L.M., F.S. and S.J.G. are supported by the Clinician Scientist Fellowship “Else Kröner Research College: 2018_Kolleg.05”.

Funding Open Access funding enabled and organized by Projekt DEAL.

Declarations

Guarantor The scientific guarantor of this publication is PD Dr. med. Roman Kloeckner.

Conflict of interest The authors declare that they have no conflict of interest.

Statistics and biometry One of the authors has significant statistical expertise.

Ethical approval Written informed consent was waived by the Institutional Review Board. This study was approved by the responsible ethics committees (Ethics Committee of the Medical Association of Rhineland Palatinate, Mainz, Germany, permit number 2021-15984).

Methodology

- retrospective
- diagnostic or prognostic study
- performed at one institution

Open Access This article is licensed under a Creative Commons Attribution 4.0 International License, which permits use, sharing, adaptation, distribution and reproduction in any medium or format, as long as you give appropriate credit to the original author(s) and the source, provide a link to the Creative Commons licence, and indicate if changes were made. The images or other third party material in this article are included in the article's Creative Commons licence, unless indicated otherwise in a credit line to the material. If material is not included in the article's Creative Commons licence and your intended use is not permitted by statutory regulation or exceeds the permitted use, you will need to obtain permission directly from the copyright holder. To view a copy of this licence, visit <http://creativecommons.org/licenses/by/4.0/>.

References

- Global Burden of Disease Liver Cancer Collaboration, Akinyemiju T, Abera S et al (2017) The burden of primary liver cancer and underlying etiologies from 1990 to 2015 at the global, regional, and national level: results from the Global Burden of Disease Study 2015. *JAMA Oncol* 3:1683–1691
- Llovet JM, Zucman-Rossi J, Pikarsky E et al (2016) Hepatocellular carcinoma. *Nat Rev Dis Prim* 2:16018
- Galle PR, Forner A, Llovet JM et al (2018) EASL clinical practice guidelines: management of hepatocellular carcinoma. *J Hepatol* 69: 182–236
- Forner A, Reig M, Bruix J (2018) Hepatocellular carcinoma. *Lancet* 391:1301–1314
- Iwakiri Y, Groszmann RJ (2014) Pathophysiology of portal hypertension. *Variceal Hemorrhage*:3–14
- Liver EAFTSOT (2012) EASL–EORTC clinical practice guidelines: management of hepatocellular carcinoma. *J Hepatol* 56: 908–943
- Bolognesi M, Merkel C, Sacerdoti D et al (2002) Role of spleen enlargement in cirrhosis with portal hypertension. *Dig Liver Dis* 34: 144–150
- Son JH, Lee SS, Lee Y et al (2020) Assessment of liver fibrosis severity using computed tomography–based liver and spleen volumetric indices in patients with chronic liver disease. *Eur Radiol* 30: 3486–3496
- Bae JS, Lee DH, Yoo J et al (2021) Association between spleen volume and the post-hepatectomy liver failure and overall survival of patients with hepatocellular carcinoma after resection. *Eur Radiol* 31:2461–2471
- Takeishi K, Kawanaka H, Itoh S et al (2018) Impact of splenic volume and splenectomy on prognosis of hepatocellular carcinoma within Milan criteria after curative hepatectomy. *World J Surg* 42: 1120–1128
- Wu W-C, Chiou Y-Y, Hung H-H et al (2012) Prognostic significance of computed tomography scan-derived splenic volume in hepatocellular carcinoma treated with radiofrequency ablation. *J Clin Gastroenterol* 46:789–795
- Dai H-T, Chen B, Tang K-Y et al (2021) Prognostic value of splenic volume in hepatocellular carcinoma patients receiving transarterial chemoembolization. *J Gastrointest Oncol* 12:1141
- Nuffer Z, Marini T, Rupasov A et al (2017) The best single measurement for assessing splenomegaly in patients with cirrhotic liver morphology. *Acad Radiol* 24:1510–1516
- Hosny A, Parmar C, Quackenbush J et al (2018) Artificial intelligence in radiology. *Nat Rev Cancer* 18:500–510
- Collins GS, Reitsma JB, Altman DG, Moons KGM (2015) Transparent reporting of a multivariable prediction model for individual prognosis or diagnosis (TRIPOD) the TRIPOD statement. *Circulation* 131:211–219
- von Elm E, Altman DG, Egger M et al (2007) The Strengthening of Reporting of Observational Studies in Epidemiology (STROBE) statement: guidelines for reporting observational studies. *Lancet* 370:1453–1457
- Müller L, Hahn F, Mähringer-Kunz A et al (2021) Immunonutritive scoring in patients with hepatocellular carcinoma undergoing transarterial chemoembolization: prognostic nutritional index or controlling nutritional status score? *Front Oncol* 11:2205
- Lammer J, Malagari K, Vogl T et al (2010) Prospective randomized study of doxorubicin-eluting-bead embolization in the treatment of hepatocellular carcinoma: results of the PRECISION V Study. *Cardiovasc Intervent Radiol* 33:41–52
- Lencioni R, De Baere T, Burrel M et al (2012) Transcatheter treatment of hepatocellular carcinoma with doxorubicin-loaded DC Bead (DEBDOX): technical recommendations. *Cardiovasc Intervent Radiol* 35:980–985
- Lencioni R, Llovet JM (2010) Modified RECIST (mRECIST) assessment for hepatocellular carcinoma. *Semin Liver Dis* 30:52–60
- Saeki I, Yamasaki T, Yamashita S et al (2020) Early predictors of objective response in patients with hepatocellular carcinoma undergoing lenvatinib treatment. *Cancers (Basel)* 12:779
- Vogel A, Merle P, Verslype C et al (2021) ALBI score and outcomes in patients with hepatocellular carcinoma: post hoc analysis of the randomized controlled trial KEYNOTE-240. *Ther Adv Med Oncol* 13:17588359211039928
- Labeur TA, Takkenberg RB, Klümpen H-J, van Delden OM (2019) Reason of discontinuation after transarterial chemoembolization influences survival in patients with hepatocellular carcinoma. *Cardiovasc Intervent Radiol* 42:230–238
- Weinmann A, Koch S, Niederle IM et al (2014) Trends in epidemiology, treatment, and survival of hepatocellular carcinoma patients between 1998 and 2009: an analysis of 1066 cases of a German HCC Registry. *J Clin Gastroenterol* 48:279–289
- Müller D, Kramer F (2021) MISenn: a framework for medical image segmentation with convolutional neural networks and deep learning. *BMC Med Imaging* 21:1–11
- Nioche C, Orhac F, Boughdad S et al (2018) LIFEx: a freeware for radiomic feature calculation in multimodality imaging to accelerate advances in the characterization of tumor heterogeneity. *Cancer Res* 78:4786–4789
- Salehi SSM, Erdogmus D, Gholipour A (2017) Tversky loss function for image segmentation using 3D fully convolutional deep networks. In: Wang Q, Shi Y, Suk HI, Suzuki K (eds) *Machine Learning in Medical Imaging. MLMI 2017. Lecture Notes in Computer Science*, vol 10541. Springer, Cham. https://doi.org/10.1007/978-3-319-67389-9_44
- Chollet F and others (2015) Keras. In: GitHub. <https://github.com/fchollet/keras>. Accessed 15 Jan 2022
- Qayyum A, Lalande A, Meriaudeau F (2020) Automatic segmentation of tumors and affected organs in the abdomen using a 3D hybrid model for computed tomography imaging. *Comput Biol Med* 127:104097
- Koitka S, Kroll L, Malamutmann E et al (2020) Fully automated body composition analysis in routine CT imaging using 3D

- semantic segmentation convolutional neural networks. *Eur Radiol*. <https://doi.org/10.1007/s00330-020-07147-3>
31. Magudia K, Bridge CP, Bay CP et al (2020) Population-scale CT-based body composition analysis of a large outpatient population using deep learning to derive age-, sex-, and race-specific reference curves. *Radiology* 298:319–329
 32. Lee C, Lee SS, Choi W-M et al (2021) An index based on deep learning-measured spleen volume on CT for the assessment of high-risk varix in B-viral compensated cirrhosis. *Eur Radiol* 31: 3355–3365
 33. Choi JW, Chung JW, Lee DH et al (2018) Portal hypertension is associated with poor outcome of transarterial chemoembolization in patients with hepatocellular carcinoma. *Eur Radiol* 28:2184–2193
 34. Scheiner B, Ulbrich G, Mandorfer M et al (2019) Short-and long-term effects of transarterial chemoembolization on portal hypertension in patients with hepatocellular carcinoma. *United European Gastroenterol J* 7:850–858
 35. Pinato DJ, Kaneko T, Saeed A et al (2020) Immunotherapy in hepatocellular cancer patients with mild to severe liver dysfunction: adjunctive role of the ALBI grade. *Cancers (Basel)* 12:1862
 36. Lee P, Chen Y, Chao Y et al (2018) Validation of the albumin-bilirubin grade-based integrated model as a predictor for sorafenib-failed hepatocellular carcinoma. *Liver Int* 38:321–330
 37. Peck-Radosavljevic M, Kudo M, Raoul J-L et al (2018) Outcomes of patients (pts) with hepatocellular carcinoma (HCC) treated with transarterial chemoembolization (TACE): Global OPTIMIS final analysis. *J Clin Oncol* 36:4018
 38. Müller L, Stoehr F, Mähringer-Kunz A et al (2021) Current strategies to identify patients that will benefit from TACE treatment and future directions a practical step-by-step guide. *J Hepatocell Carcinoma* 8:403
 39. Sacco R, Bargellini I, Bertini M et al (2011) Conventional versus doxorubicin-eluting bead transarterial chemoembolization for hepatocellular carcinoma. *J Vasc Interv Radiol* 22:1545–1552
 40. Golfieri R, Giampalma E, Renzulli M et al (2014) Randomised controlled trial of doxorubicin-eluting beads vs conventional chemoembolisation for hepatocellular carcinoma. *Br J Cancer* 111:255–264
 41. Kloeckner R, Weinmann A, Prinz F et al (2015) Conventional transarterial chemoembolization versus drug-eluting bead transarterial chemoembolization for the treatment of hepatocellular carcinoma. *BMC Cancer* 15:465

Publisher's note Springer Nature remains neutral with regard to jurisdictional claims in published maps and institutional affiliations.